PERGAMON

International Journal of Rock Mechanics and Mining Sciences 37 (2000) 317–336

International Journal of Rock Mechanics and Mining Sciences

www.elsevier.com/locate/ijrmms

Constraining the stress tensor in the Visund field, Norwegian North Sea: Application to wellbore stability and sand production

D. Wiprut*, M. Zoback

Department of Geophysics, Stanford University, Stanford, CA 94305-2215, USA

Accepted 7 October 1999

Abstract

In this study we examine drilling-induced tensile wellbore failures in five exploration wells in the Visund oil field in the northern North Sea. We use observations of drilling-induced wellbore failures as well as density, pore pressure, and leak-off test measurements to estimate the magnitudes and orientations of all three principal stresses. Each well yields a very consistent azimuth of the maximum horizontal stress ($100° \pm 10°$), both with depth and laterally across the field. Stress orientations are constrained at depths as shallow as 2500 m and as deep as 5300 m in these wells. We show that the magnitudes of the three principal stresses (S_v, S_{hmin}, and S_{Hmax}) are also consistent with depth and reflect a strike-slip to reverse faulting stress regime. The magnitude of the maximum horizontal stress is shown to be significantly higher than the vertical and minimum horizontal stresses (e.g. $S_v = 55$ MPa, $S_{hmin} = 53$ MPa, and $S_{Hmax} = 71.5$ MPa at 2.8 km depth). Data from earthquake focal plane mechanisms (Lindholm et al., 1995, Proceedings of the Workshop on Rock Stresses in the North Sea, Trondheim, Norway [1]) show similar stress orientations and relative magnitudes and thus indicate a stress field that is relatively consistent throughout the thickness of the brittle crust.

We illustrate how knowledge of the full stress tensor allows one to place bounds on in situ rock strength and determine optimally stable trajectories for wellbore stability and sand production during drilling, after the completion of drilling, and as pore pressure is reduced during oil and gas production.

1. Introduction

Determination of the full stress tensor in oil fields is critical for addressing engineering problems of wellbore stability and sand production as well as geologic problems such as understanding dynamic constraints on hydrocarbon migration and fracture permeability. Controlling wellbore instabilities requires understanding of the interaction between the rock strength and in situ stress. Because in situ stress and rock strength cannot be altered or controlled, the only way to inhibit wellbore failure during drilling is to adjust engineering practice by choosing optimal trajectories and mud weights. Similarly, utilization of an appropriate trajectory can limit sand production by reducing the tendency for failure around a wellbore.

This paper presents an analysis of stress and wellbore stability in the Visund field, which is located in the Norwegian North Sea to the northwest of Bergen, near the western edge of the Viking Graben (Fig. 1). The Visund field sits within the approximately 25 km long, 2.5 km wide Visund fault-block, which is the most easterly major fault block on the Tampen Spur [2]. The state of stress in the Norwegian North Sea is generally characterized by an east–west to northwest–southeast compression, but exhibits appreciable scatter in places (e.g., Müller et al. [3]; Lindholm et al. [1]).

In the following sections we describe how observations of drilling-induced compressive failures (e.g.,[4–6]) and wellbore tensile failures (e.g. [7–10]) can be integrated with other routinely available wellbore information to constrain the full stress tensor.

* Corresponding author. Tel.: +1-650-725-6072; fax: +1-650-725-7244.

E-mail address: wiprut@pangea.stanford.edu (D. Wiprut).

1365-1609/00/$ - see front matter
PII: S1365-1609(99)00109-4

Our approach follows an integrated stress measurement strategy (ISMS), outlined by Zoback et al. [11], and Brudy et al. [12], to constrain the magnitudes and orientations of all three principal stresses. Using our estimates of in situ stress we place bounds on the effective rock strength. This information is then used to determine optimally-stable trajectories for drilling and minimizing sand production.

2. Observations of wellbore failure

Examination of Formation MicroScanner/Formation MicroImager (FMS/FMI) logs [13] provided by Norsk Hydro, and run in seven wells, revealed extensive drilling-induced tensile failures in five of the wells. Examples of this data can be seen in Appendix A. We plot the azimuth of the tensile fractures as a function of depth in Fig. 2. In each case, black data points represent tensile fractures that are aligned with the axis of the wellbore, and data points representing tensile fractures that are inclined with respect to the axis of the wellbore are shown in gray. Error bars for near-axial tensile failures show the variation in azimuth of each fracture; while error bars for inclined tensile failures show the portion of the wellbore circumference spanned by each fracture. Near the center of each plot, bit trips and "wash and ream" operations are shown by horizontal and vertical lines respectively. A bit trip is plotted each time the drill string is run into the hole. This operation may cause a significant rise in the mud pressure at the bottom of the hole due to a piston effect. Washing and reaming the hole involves scraping the hole clean, and may remove evidence of drilling-induced tensile fractures. There is no visible correlation between the occurrence (or absence) of tensile fractures and these special drilling operations, suggesting that the tensile fractures formed (or did not form) during normal drilling operations, rather than as a result of extreme conditions in the well such as tripping the bit or reaming the hole.

All wells except 10 S were drilled nearly vertically to total depth. Near-axial tensile fractures in wells 6, 7, 8, and 11, as well as in the vertical portion of 10 S, suggest that the vertical and two horizontal stresses are principal stresses in this field [9]. Inclined tensile fractures observed in four of the wells (most prevalent in the 10 S well) indicate possible exceptions to this and are discussed in Appendix B.

In order to determine the orientation of the stress field in this region, we focus on the orientation of the tensile fractures aligned with the wellbore axis. We use

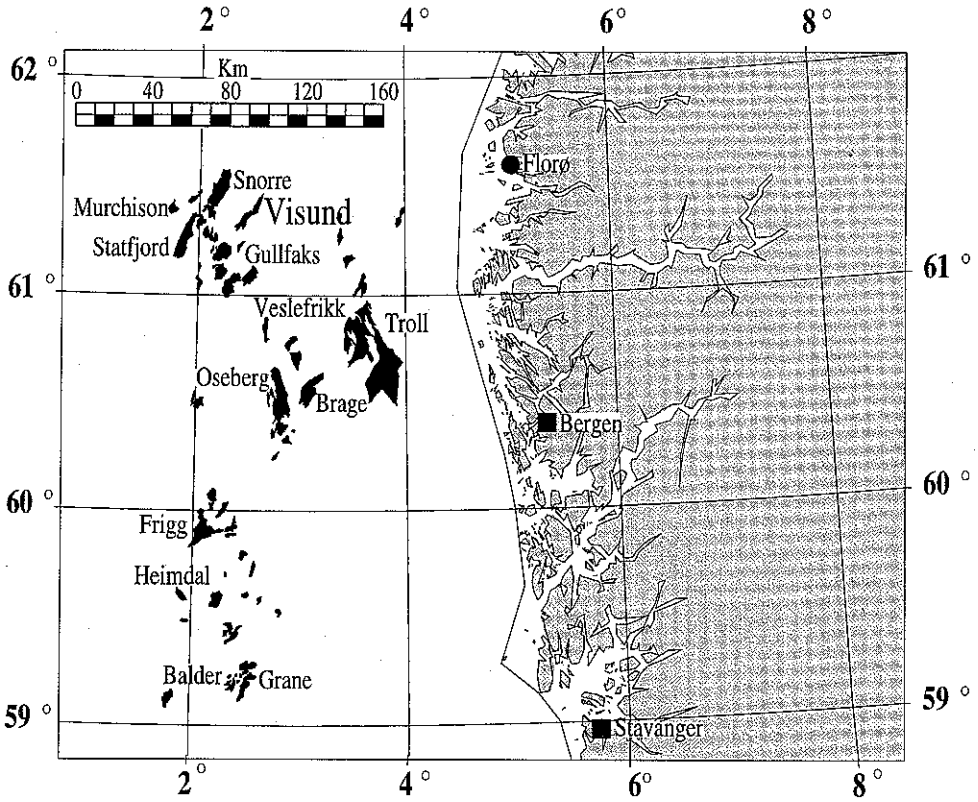

Fig. 1. Map of the northern North Sea modified from the Norwegian Petroleum Directorate, 1997. The Visund field sits on the western edge of the Viking Graben to the northwest of Bergen, Norway.

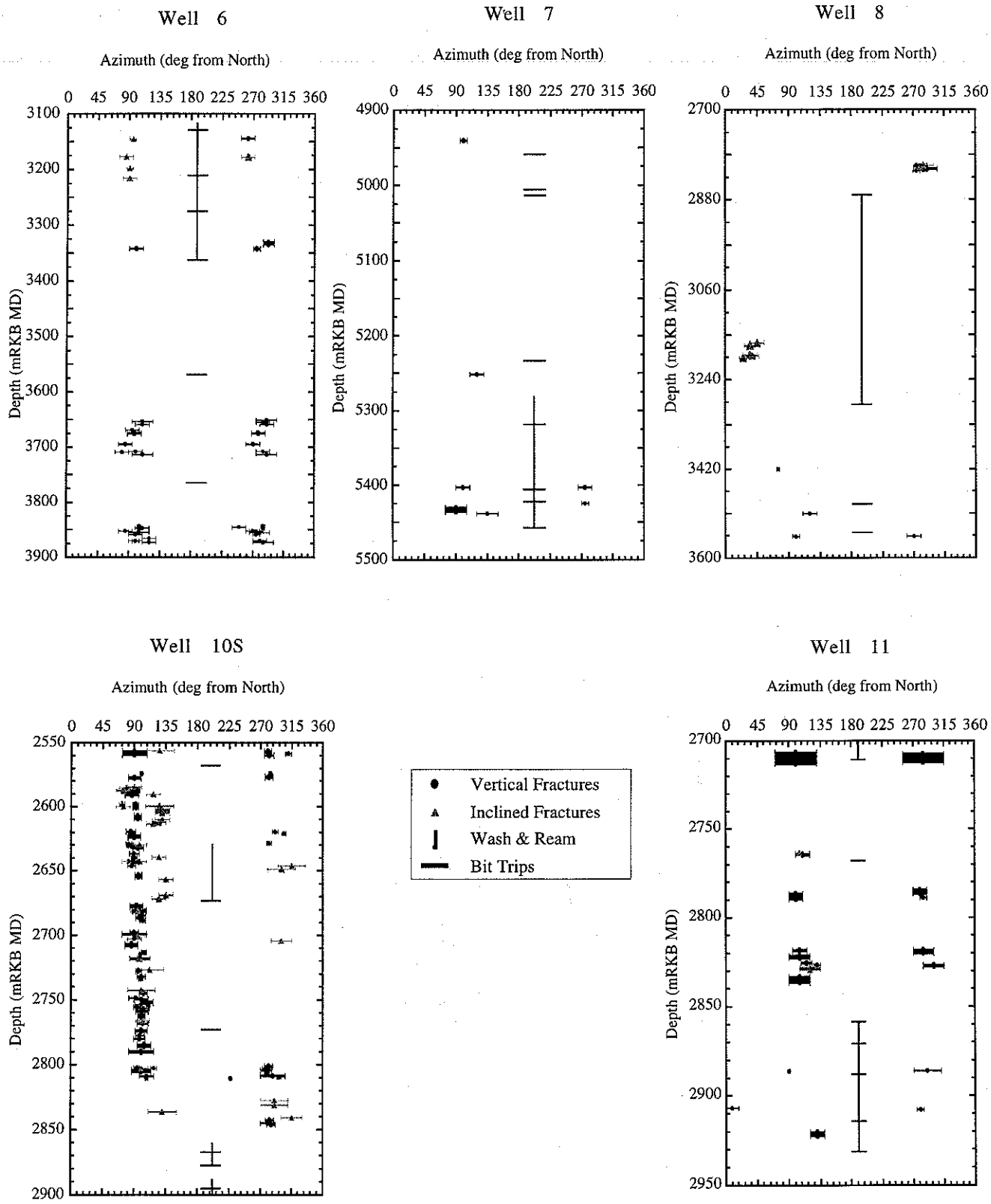

Fig. 2. Azimuth of drilling induced tensile fractures observed in image logs as a function of depth.

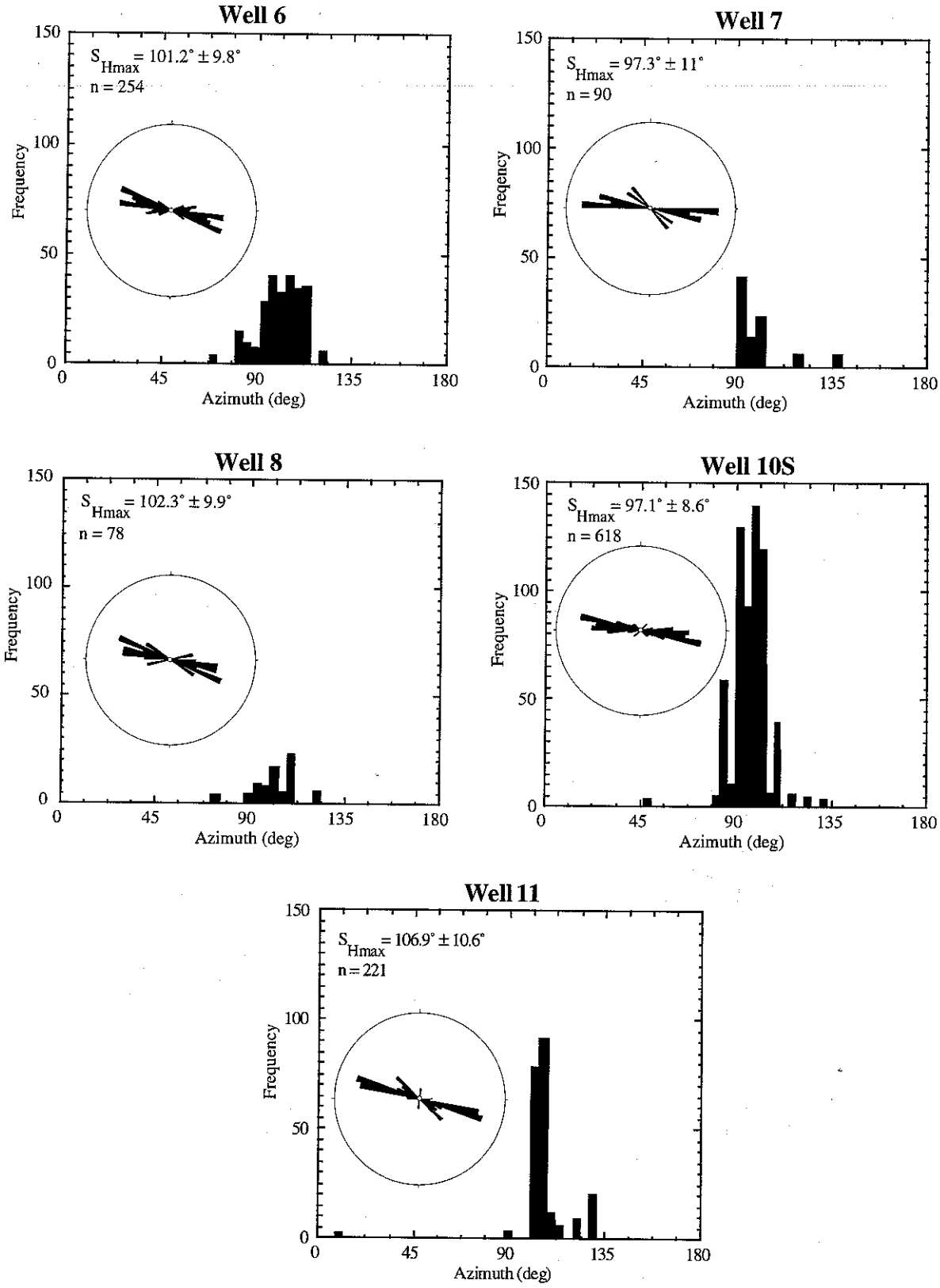

Fig. 3. Histograms and rose diagrams showing the orientation of the maximum horizontal stress. Each rose plot is normalized by the number of data points, and therefore the length of the bars does not reflect the relative frequency of the tensile fractures between wells. The number of 0.2 m observations (n) is shown in each case. The statistics follow Mardia [14].

a circular statistical method developed by Mardia [14] to obtain the mean azimuth and standard deviation of the maximum horizontal stress for each well (insets of Fig. 3). The uncertainty in the azimuth represents two standard deviations from the mean. The frequency is calculated by adding the tensile fractures in 0.2 m intervals.

An anomalous stress orientation seen from a wellbore breakout (reported by Fejerskov [15] and later analyzed in this study) and inclined tensile fractures was detected over an approximately 135 m interval of well 8. This stress orientation was not seen in any of the other wells to the north or south, and appears to be the result of a localized stress anomaly due to slip

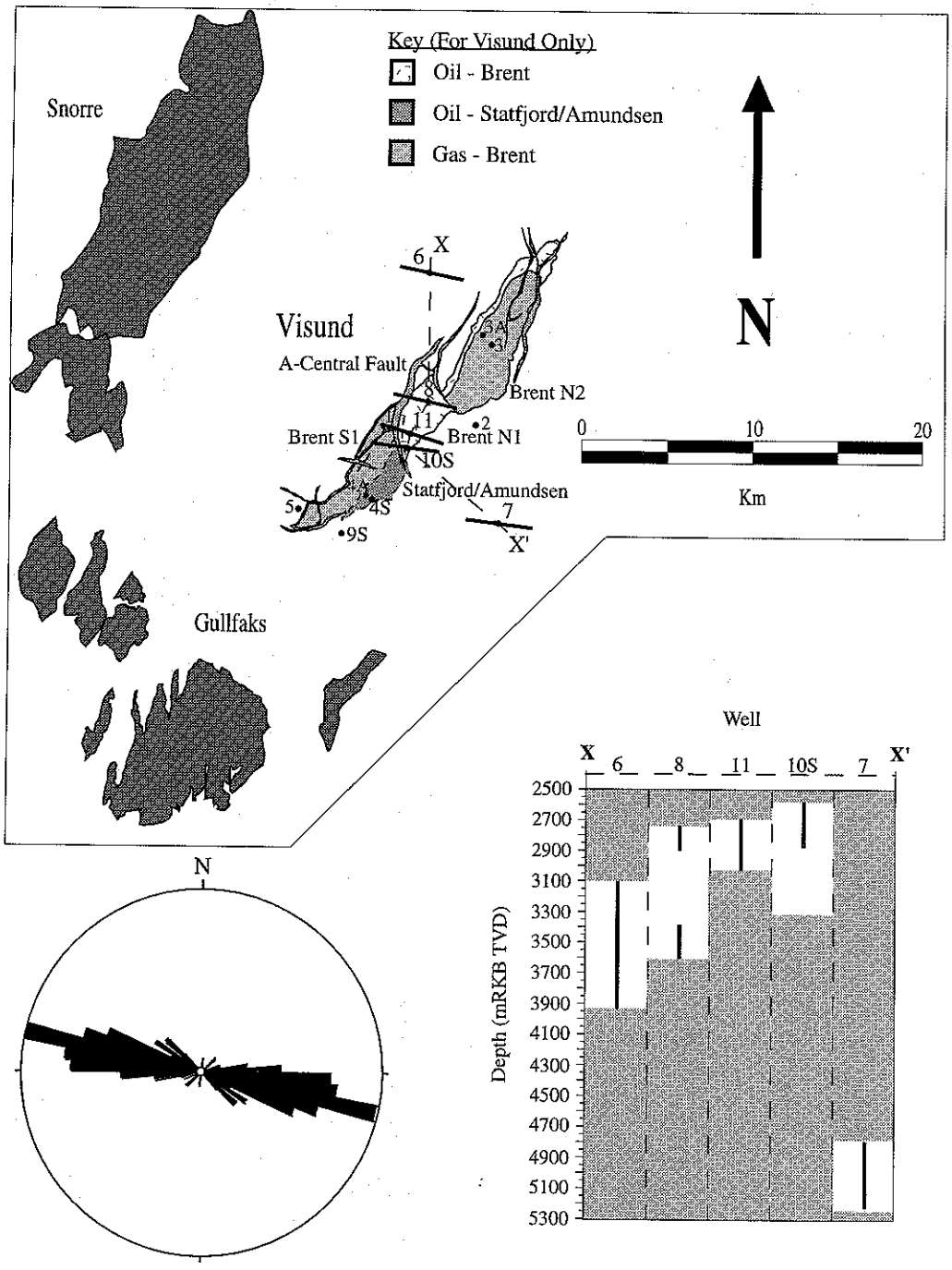

Fig. 4. Map view of S_{Hmax} orientations (modified from Norwegian Petroleum Directorate and Norsk Hydro maps), rose plot with all of the orientation data, and plot showing the depths over which S_{Hmax} is constrained in each well. The gray regions show portions of the wells that were not logged. The orientation of the maximum horizontal stress is consistent both laterally and with depth in this field.

on a preexisting fault penetrated by this well. The subseismic fault responsible for this anomaly can be inferred from the geologic section by noting a repeated sequence of the Brent reservoir sands. The relationship between anomalous stress fields and slip on faults has been noted by other authors (e.g. [16–18]). We therefore assume that this single anomaly is not representative of the tectonic stress field.

Fig. 4 summarizes our findings concerning the orientation of the maximum horizontal stress. The mean orientation of S_{Hmax} for each well is plotted in map view and clearly shows a consistently oriented stress field. The rose diagram shows the orientations of all of the tensile fractures from all of the wells. The plot in the lower right shows the depths over which the orientation of S_{Hmax} is constrained in each well. Gray shaded regions show portions of each well that were not logged. This plot shows that the maximum horizontal stress is constrained to depths as shallow as 2550 m and as deep as 5250 m (RKB TVD). The orientation of the maximum horizontal stress as determined from earthquake focal plane mechanisms [1] is similar to our findings (azimuths between 90° and 120°). Our data, coupled with these findings, indicate that the orientation of the maximum horizontal stress is consistent across the Visund field as well as throughout the thickness of the brittle crust.

The scatter in stress directions observed in some parts of the northern North Sea (determined from wellbore elongations) has led some investigators to conclude that shallow stress directions are decoupled from the deeper regional stress field (e.g. [19]). We have shown that close examination of reliable data reveals a consistently oriented stress field, and we further demonstrate in Appendix B that we can use this stress field to explain the occurrence of inclined drilling-induced tensile fractures.

3. In situ stress and rock strength

We utilize the interactive software package, Stress and Failure of Inclined Boreholes (SFIB), developed by Peska and Zoback [20], to constrain the maximum horizontal stress magnitudes and to put limits on rock strength. Estimation of the maximum horizontal stress requires prior knowledge of the vertical stress, the minimum horizontal stress, the pore pressure, the mud weight, and the change in temperature at the wellbore wall during drilling. Final well reports provided by Norsk Hydro contain this information. We analyze each well individually so that estimates of the maximum horizontal stress are not affected by data from wells in different pore pressure compartments or with slightly differing overburden stresses. The vertical stress, S_v, used in this study was derived from integrated density logs. Because these logs are seldom run up to the sea floor, the density must be estimated in the shallow subsurface. The resulting errors in the overburden gradient are negligible in wells 10 S and 11 since only a small amount (approximately 50 m) of sediment is not accounted for by the density logs. In wells 6, 7, and 8, the density logs were only run in the deeper portions (below approximately 2500 m) of the holes. The densities used in the upper portions of these holes are estimated from shallow measurements in nearby holes. Overburden gradients from wells 6, 7, and 8 nevertheless provide overburden stresses which are similar to those found in wells 10 S and 11. We derive the minimum horizontal stress, S_{hmin}, from Leak-off Tests (LOT) and Formation Integrity Tests (FIT) conducted in each well (see Gaarenstroom et al. [21]). In all of the wells the depth at which we wish to constrain the maximum horizontal stress is below the deepest LOT or FIT. We therefore assume a linear stress gradient between LOTs in each well and extrapolate this trend to the depth of investigation. The pore pressure, P_p, was obtained from Repeat Formation Tests (RFT). In order to use a reliable pore pressure value the stress analysis in each well was conducted as close as possible to an RFT depth. Pore pressure data was not available for well 7. Consequently, we do not constrain the maximum horizontal stress in this well. We derive a mud weight value, P_m, from the maximum equivalent circulating density (ECD), which takes into account frictional effects between the wellbore wall and the mud as well as the mud density. We use a static mud weight in well 6 because an ECD value was unavailable. Use of the highest mud density value is required since it is impossible to determine the precise mud weight at which the tensile cracks initiated. Although the tensile fractures may have formed at mud pressures lower than the ones we use, our utilization of the highest mud pressure allows us to calculate a reasonable lower bound for the maximum horizontal stress. An upper bound for the maximum horizontal stress is derived from our analysis of rock strength and compressive failures in these wells. The amount of cooling at the wellbore wall was derived from temperature gradient plots. Each well showed cooling between 20° and 30°C at the depths of investigation. While the temperature change of the wellbore wall was considered in these calculations, it had little effect on the estimation of S_{Hmax}.

Fig. 5 shows the analysis for the maximum horizontal stress, S_{Hmax}. The plots represent the allowable stress state at a given depth constrained by: (1) Mohr–Coulomb frictional faulting theory for the crust assuming a coefficient of sliding friction of 0.6 [22] (four sided polygon); and (2) compressive and tensile wellbore wall failures (thick short dashes and long dashes respectively) (see Moos and Zoback [8], for an expla-

nation). Stress magnitudes that fall above the short dashed tensile failure contour (assumed to be zero in this study) indicate stress states consistent with the occurrence of drilling-induced tensile fractures, while values that fall below indicate no tensile failures should occur. Similarly, for a given rock strength, stress magnitudes that fall above one of the long dashed compressive failure contours indicate breakouts should occur, while those that fall below indicate no breakouts should be observed. We constrain the maximum horizontal stress only where tensile fractures were observed in each of these wells, meaning the stress state must be such that it falls above the short dashed tensile failure line in our figures. No breakouts were observed in any of the wells at the depths where we constrain the maximum horizontal stress. This observation is utilized below to place a lower bound on the in situ rock strength. While coefficients of sliding friction may be as high as 1.0 in some rocks, faults in sediments tend to have lower coefficients of friction. We consider a coefficient of friction of 0.6 to be an upper bound in this case, as the sediments are poorly cemented and consolidated.

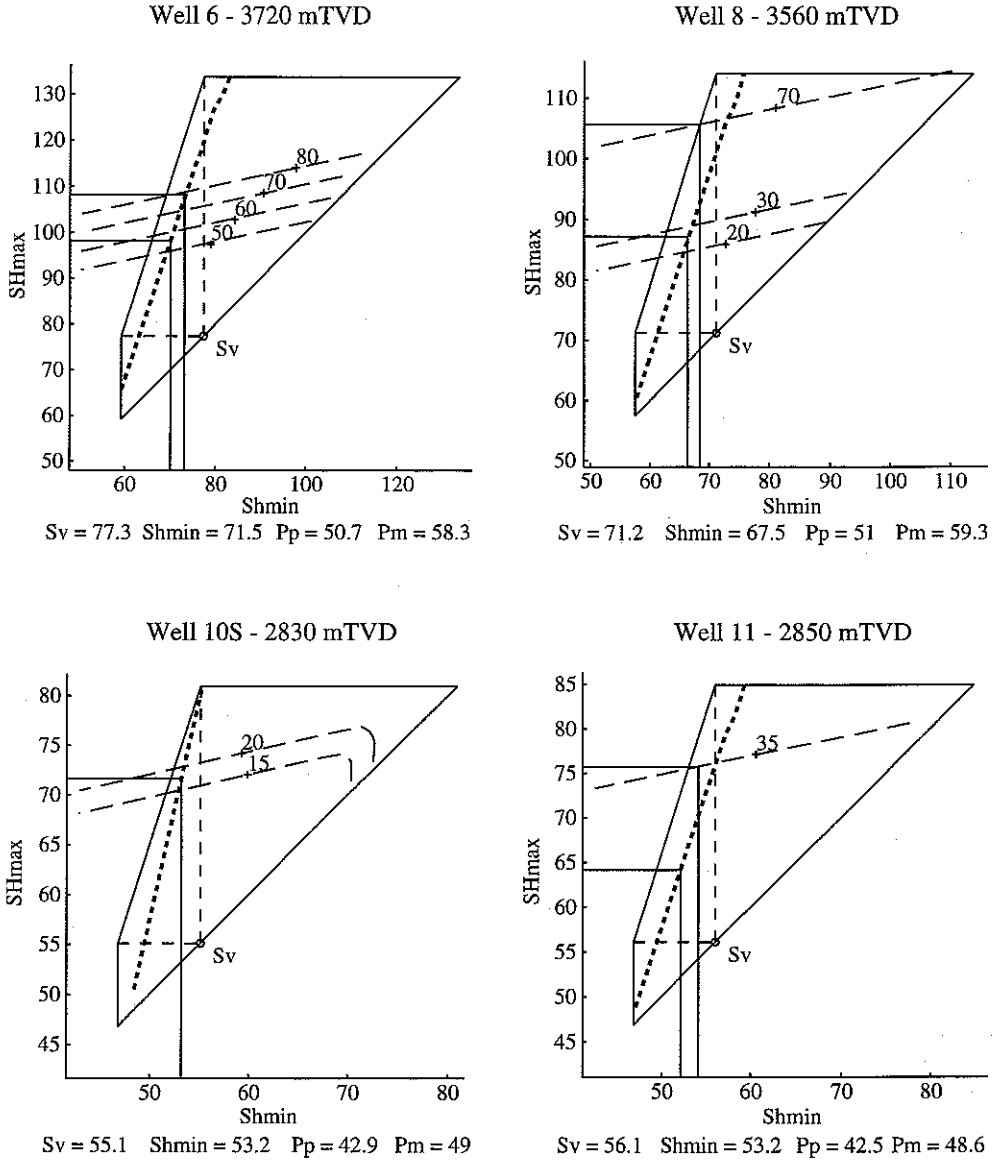

Fig. 5. Stress polygons showing the constrained values of the maximum horizontal stress in each of the wells. Each analysis is developed for a specific depth shown above the figure. The relevant stress inputs (in MPa) are shown below the figures. Tensile failure contours are thick short dashes, and breakout contours are long dashes. Each breakout line represents a different rock strength value, as shown, assuming that a breakout width of at least 40° would be required in order to be detected by the wide pads of the FMI tool.

3.1. Constraining S_{Hmax} in wells 10 S and 11

Wiprut et al. [23] presented a stress analysis of well 10 S using near-axial tensile fractures. The points of departure of this study from the previous study are three-fold: (1) we constrain the maximum horizontal stress in multiple wellbores; (2) we perform a more comprehensive analysis of in situ rock strength; (3) we analyze inclined tensile fractures observed in well 10 S.

Well 10 S presents the best opportunity to reliably constrain the magnitude of the maximum horizontal stress. As the well increases in deviation and begins to encounter a different stress field a transition from a stress state in which tensile fractures form, to one in which they do not, occurs. Fig. 6 shows that tensile fractures form continuously in this well to a deviation of approximately 35°, and then abruptly stop. Because tensile failures are present at the depth of investigation, and the tensile cracks stop just below 2830 mTVD (as shown in Fig. 6), we expect the value of S_{Hmax} at 2830 m to be approximately equal to the value indicated by the short dashed contour line (71.5 ± 4.5 MPa) (Fig. 5). The steep slope of the short dashed tensile failure lines in Fig. 5 means a small uncertainty in the minimum horizontal stress creates a large uncertainty in the maximum horizontal stress. We illustrate in Appendix B that the occurrence of inclined tensile fractures is easily explained by this stress tensor, using only minor (±10°) perturbations to the mean orientation of the stress tensor and slight increases in the mud pressure.

Each compressive failure contour in Fig. 5 represents a different uniaxial compressive rock strength (UCS) value, as shown, assuming that a breakout width of at least 40° would be required in order to be detected by the wide pads of the FMI tool. Well 10 S

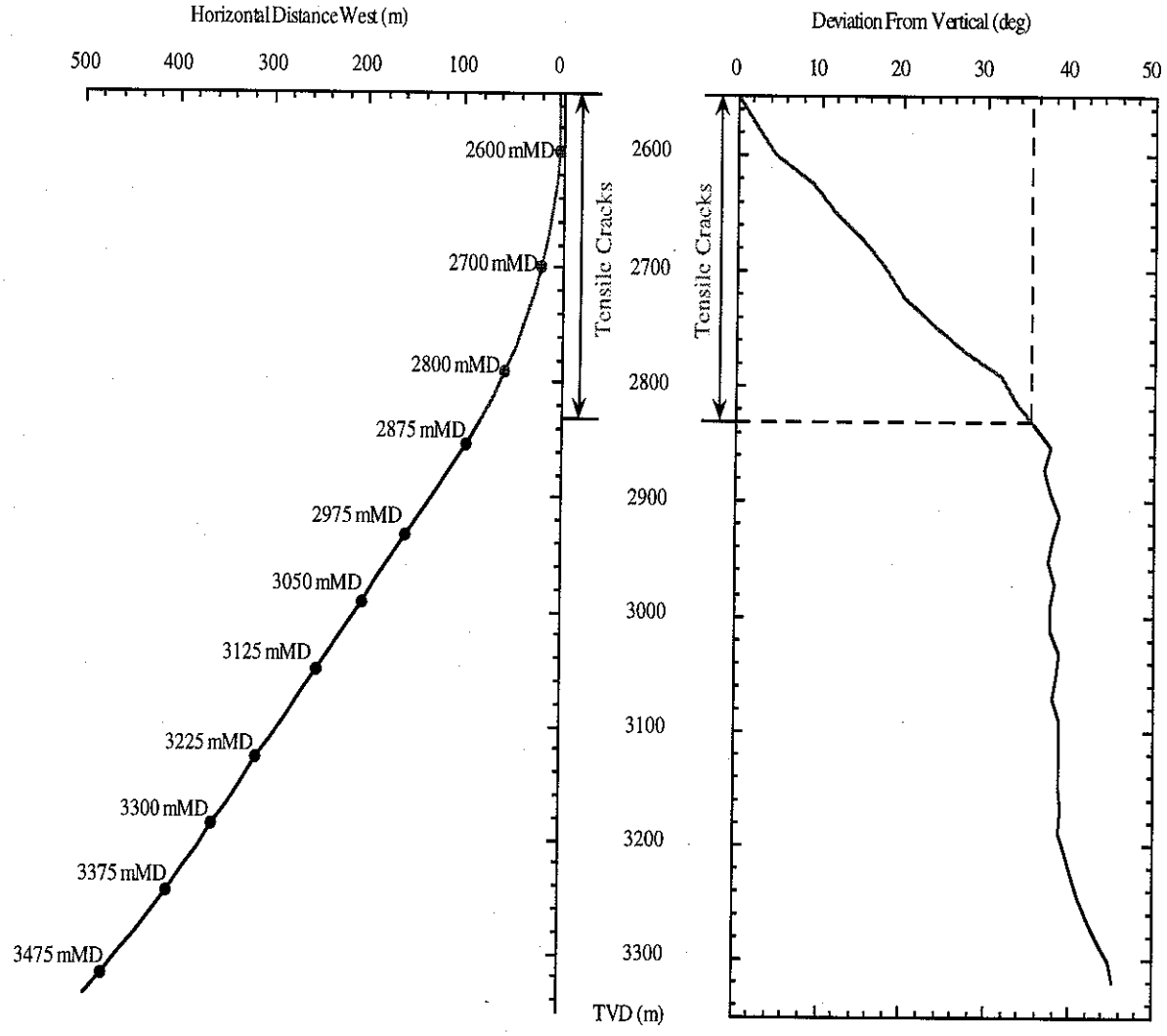

Fig. 6. Section view of the drilling direction (left) and wellbore deviation as a function of depth (right). Measured depths are plotted along the wellbore path. Tensile fractures were detected from 2550 to 2850 m measured depth (2550–2830 m true vertical depth). The tensile fractures stopped at a deviation of 35° at 2830 mTVD.

is the only well in which knowledge of the rock strength is not needed to constrain S_{Hmax} because the stress is constrained by the tensile failure contour. Since no breakouts were detected in this well, the stress values determined above imply the apparent UCS of the rock (assuming a coefficient of internal friction of about 1.0) is greater than 18 MPa. Laboratory strength measurements conducted by Norsk Hydro on cores taken throughout the region give an average value for the uniaxial compressive rock strength of approximately 25 MPa in the caprocks at this depth. The rock strength may also be constrained by the breakout width if breakouts occur, as weak rock will have wider breakouts than strong rock [5].

In well 11 we use a reasonable upper bound on uniaxial compressive rock strength derived from laboratory tests on core, the upper bound of the minimum horizontal stress, and the lack of breakouts at this depth, in order to constrain the upper bound for the maximum horizontal stress. Since the upper bound on the rock strength determined from the Norsk Hydro laboratory tests on core is approximately 35 MPa at this depth, and in this formation, the maximum horizontal stress must fall below the 35 MPa breakout line. We use the lower bound of S_{hmin}, with the tensile failure contour, to constrain the lower bound of S_{Hmax}. The mean value from this range is our assumed value of S_{Hmax}, and the range is the uncertainty (70 ± 6 MPa) (Fig. 5).

3.2. Constraining S_{Hmax} in wells 6 and 8

In well 6, the least principal stress at the depth of interest is 71.5 ± 1.5 MPa. To account for the existence of drilling-induced tensile fractures, this requires lower bound values of S_{Hmax} to be 103.5 ± 5.5 MPa (Fig. 5). As there are no breakouts observed in this well, these values imply UCS values that exceed 50–80 MPa. While laboratory UCS tests done on the Etive sands (which occur only 5 m below the depth at which the stress analysis is done in well 6) indicate maximum strengths of only 30 MPa, the sandstone at the depth analyzed is more well cemented with silica than is the Etive. A theoretical estimate of strength in clean arenites provides a potential strength of 90 MPa for an average porosity of 15% [24]. Although the sandstone in question is not clean, it is reasonable to assume that the UCS is 50–80 MPa. We assume that the lower bound value of S_{Hmax} (103.5 ± 5.5 MPa) is approximately correct because if the value were even slightly higher (as permitted by Coulomb faulting theory, Fig. 5), the corresponding rock strengths would be unreasonably high.

In well 8 the upper bound of the maximum horizontal stress is constrained using the upper bound of S_{hmin} and Coulomb faulting theory. Since no breakouts were observed in this well at 3560 mTVD, the upper bound values of S_{hmin} and S_{Hmax} predict that the rock strength is greater than 70 MPa. In this well we use the lower bound of S_{Hmax} as our assumed value of the maximum horizontal stress, and the upper bound as the extent of our uncertainty since both the rock strength and the friction coefficient may be either higher or lower than shown in the figure. The maximum horizontal stress in well 8 is constrained to be 105 MPa S_{Hmax} 87 MPa (Fig. 5) although the upper bound is only limited by the assumed frictional strength of the crust.

Fig. 7 shows a summary of our stress results for the Visund field. We compiled overburden, LOT, and RFT data from all 13 wells drilled in the Visund field. Each data point in this plot is derived as strictly as possible from the most reliable data from each well. The data for the minimum horizontal stress is derived from our analysis of leak-off test curves. Reported leak-off tests without pressure–time curves are not considered in this compilation. The well number is shown next to each data point. The vertical stress is derived using an overburden gradient averaged across the entire field. Small differences in the overburden gradients were detected, but the resulting stress profiles from these gradients were sufficiently similar such that we could neglect any differences. The pore pressure data is compiled from RFTs conducted in all of the wells in the field. Our constrained values for the maximum horizontal stress are shown in gray.

Note that the maximum horizontal stress is significantly larger than the vertical and minimum horizontal stresses, contrary to what other studies have found [25]. However, our stress magnitudes are consistent with the strike-slip to reverse faulting stress field observed from earthquake focal plane mechanisms in the North Sea [1]. Further evidence of recent reverse faulting deformation was seen in sub-seismic faults inferred from repeated sequences of Brent sands in the lithology logs of several wells. The existing deformation data therefore supports our prediction of high horizontal stresses in this region of the North Sea.

Table 1 provides a summary of the stress data found in each of the seven wells. Wells 4A and 4 S did not have any interpretable tensile fractures as a result of poor image quality and low wellbore coverage. The tensile fractures observed in well 7 appear at depths far below any pore pressure or leak-off test measurements. We therefore do not provide estimates of stress magnitudes in well 7.

4. Application to wellbore stability

Exploratory wells drilled in Visund prior to the spudding of well 10 S frequently encountered drilling

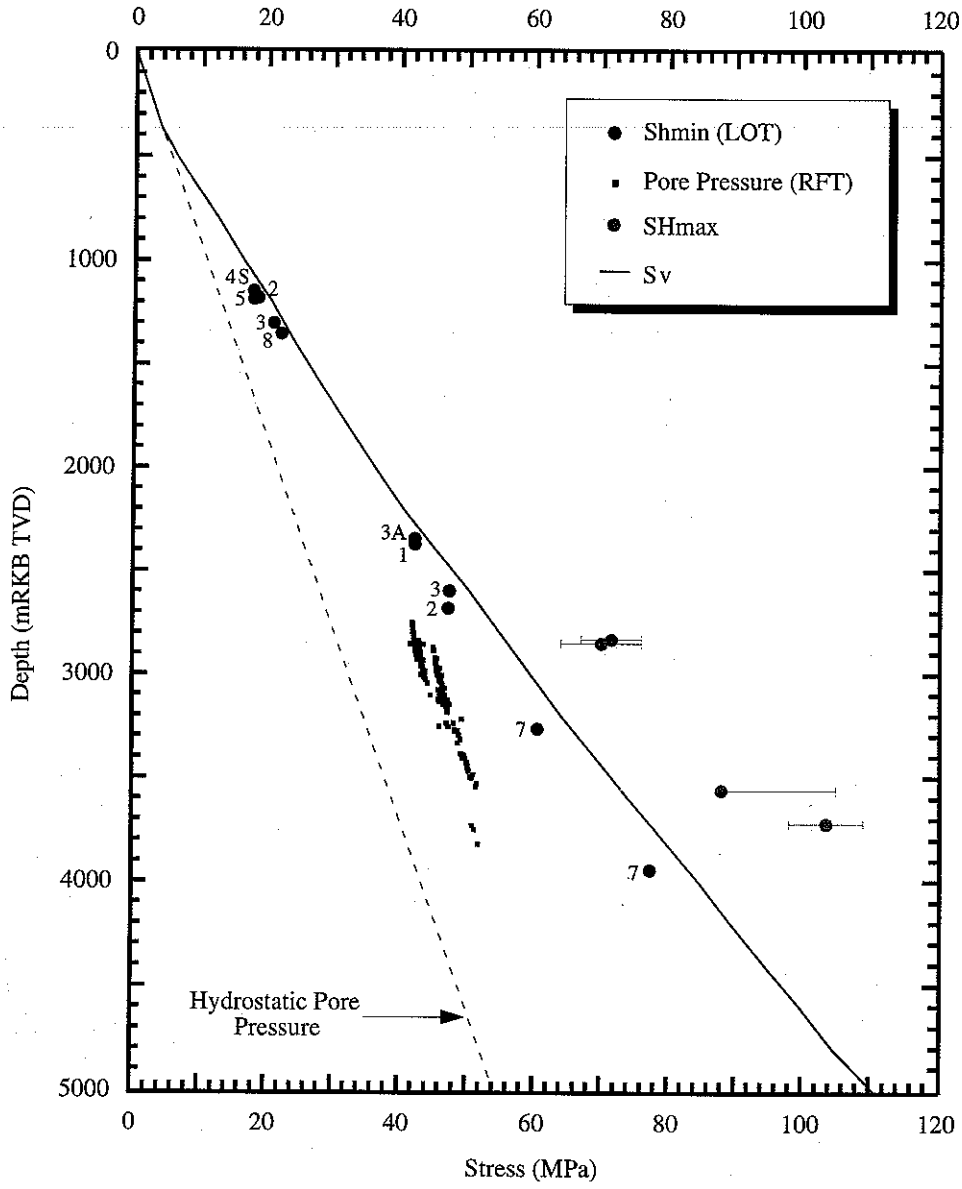

Fig. 7. Stress vs depth in Visund. Each stress point in this plot is derived as strictly as possible from the most reliable data in the field. Each leak-off test data point shows the well in which the test was run.

Table 1

Well	Log	SH Azimuth	Depth (mTVD)	SH Magnitude (MPa)	Sh Magnitude (MPa)	Sv Magnitude (MPa)
4A	FMS	–	–	–	–	–
4 S	FMS	–	–	–	–	–
6	FMS	101.2° ± 9.8°	3720	103.5 ± 5.5	71.5 ± 1.5	77.3
7	FMS	97.3° ± 11°	–	–	–	–
8	FMI	102.3° ± 9.9°	3560	87 + 18	67.5 ± 1	71.2
10 S	FMI	97.1° ± 8.6°	2830	71.5 ± 4.5	53.2 ± 1	55.1
11	FMI	106.9° ± 10.6°	2850	70 ± 6	53.2 ± 1	56.1

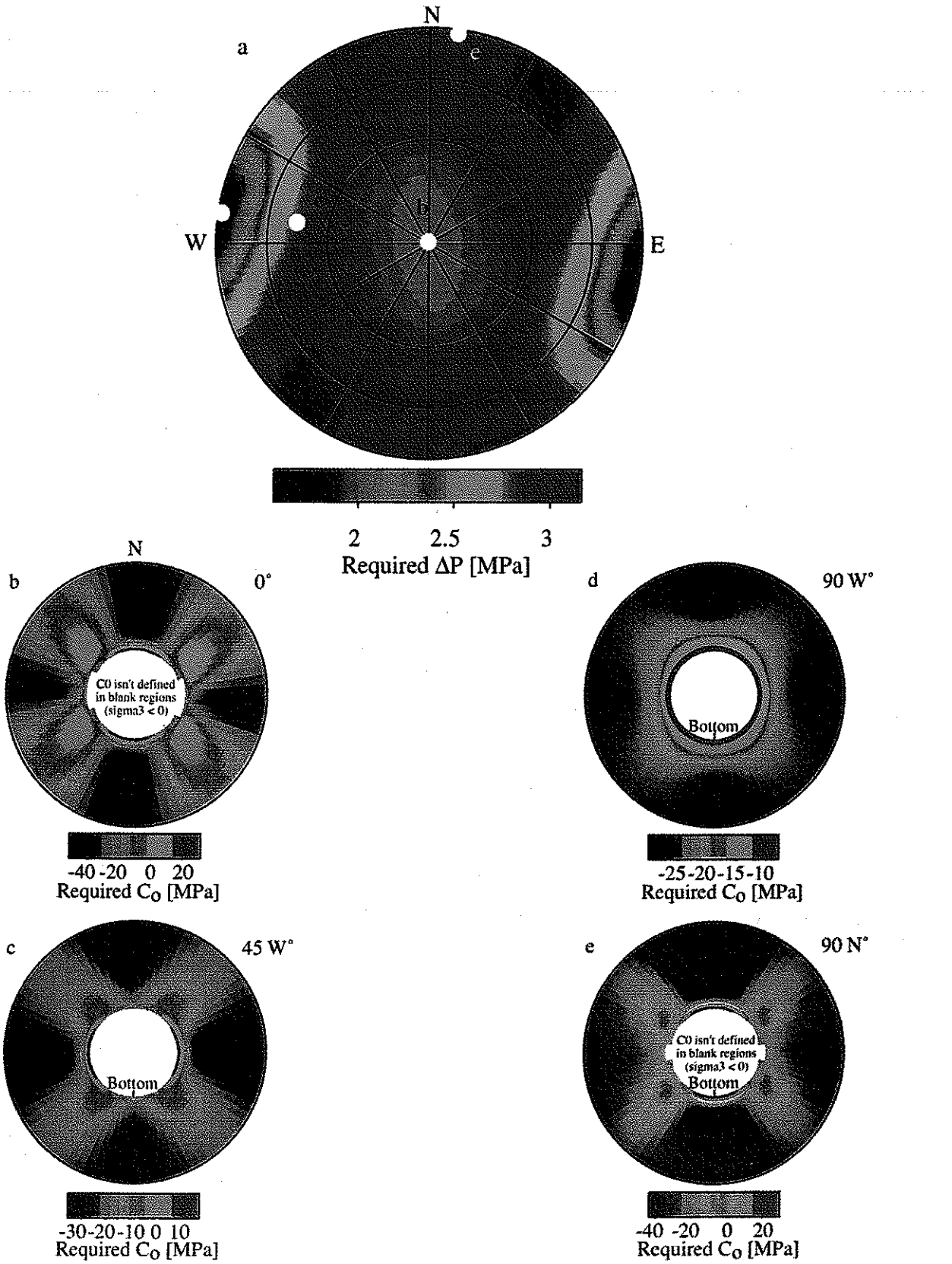

Fig. 8. (a) Stereonet showing the differential pore pressure needed to prevent compressive wellbore failures during drilling. The white points show the orientations of the wellbore cross-sections shown in parts (b–e). The colors correspond to the compressive rock strength needed to prevent failure in different parts of the rock surrounding the hole. (b) Vertical well. (c) Well inclined 45° at an azimuth of 280°. (d) Horizontal well drilled toward S_{Hmax}. (e) Horizontal well drilled toward S_{hmin}.

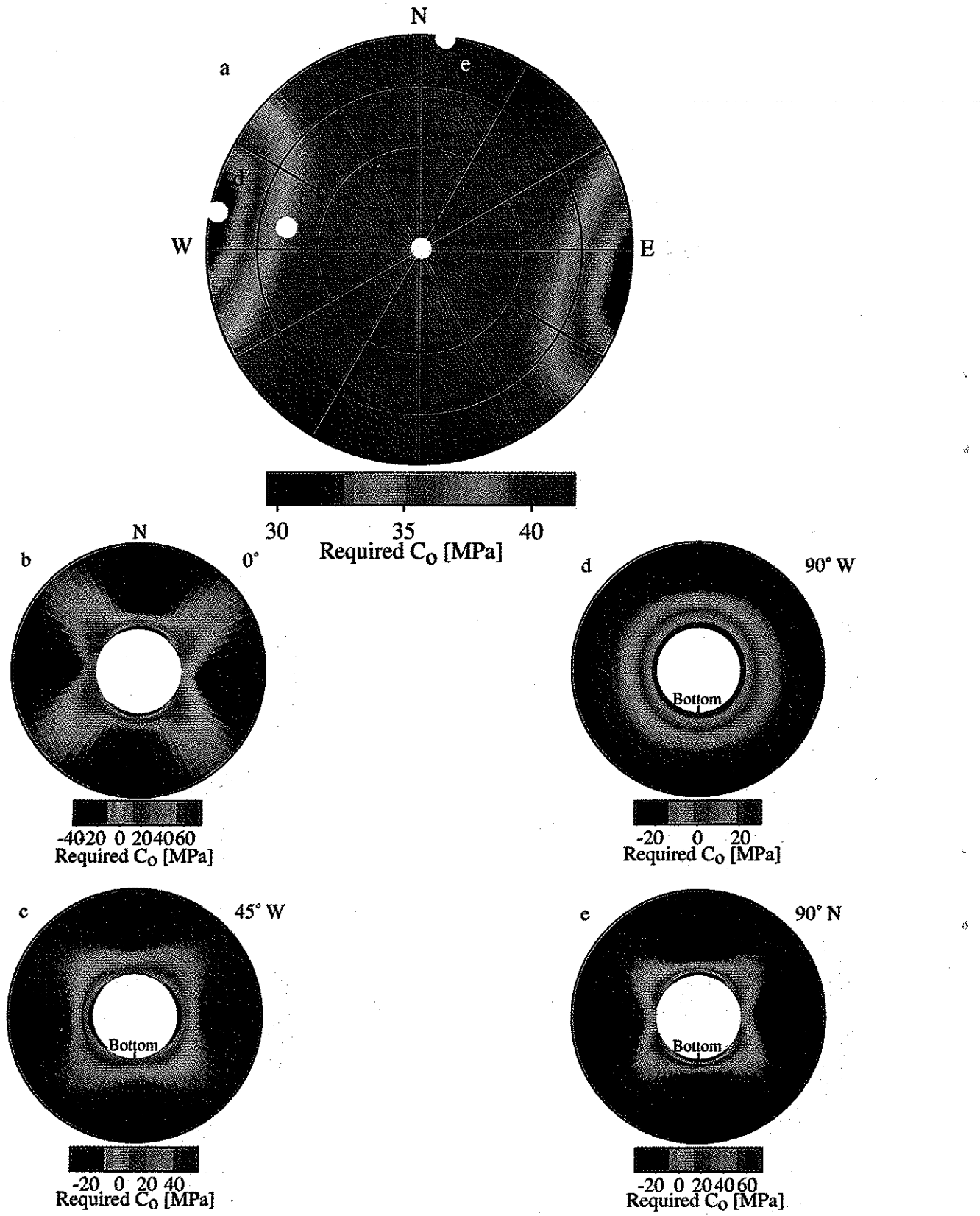

Fig. 9. (a) Stereonet showing the compressive rock strength needed to prevent wellbore failures after the completion of drilling. The white points show the orientations of the wellbore cross-sections shown in parts (b–e). The colors correspond to the compressive rock strength needed to prevent failure in different parts of the rock surrounding the hole. (b) Vertical well. (c) Well inclined 45° at an azimuth of 280°. (d) Horizontal well drilled toward S_{Hmax}. (e) Horizontal well drilled toward S_{hmin}.

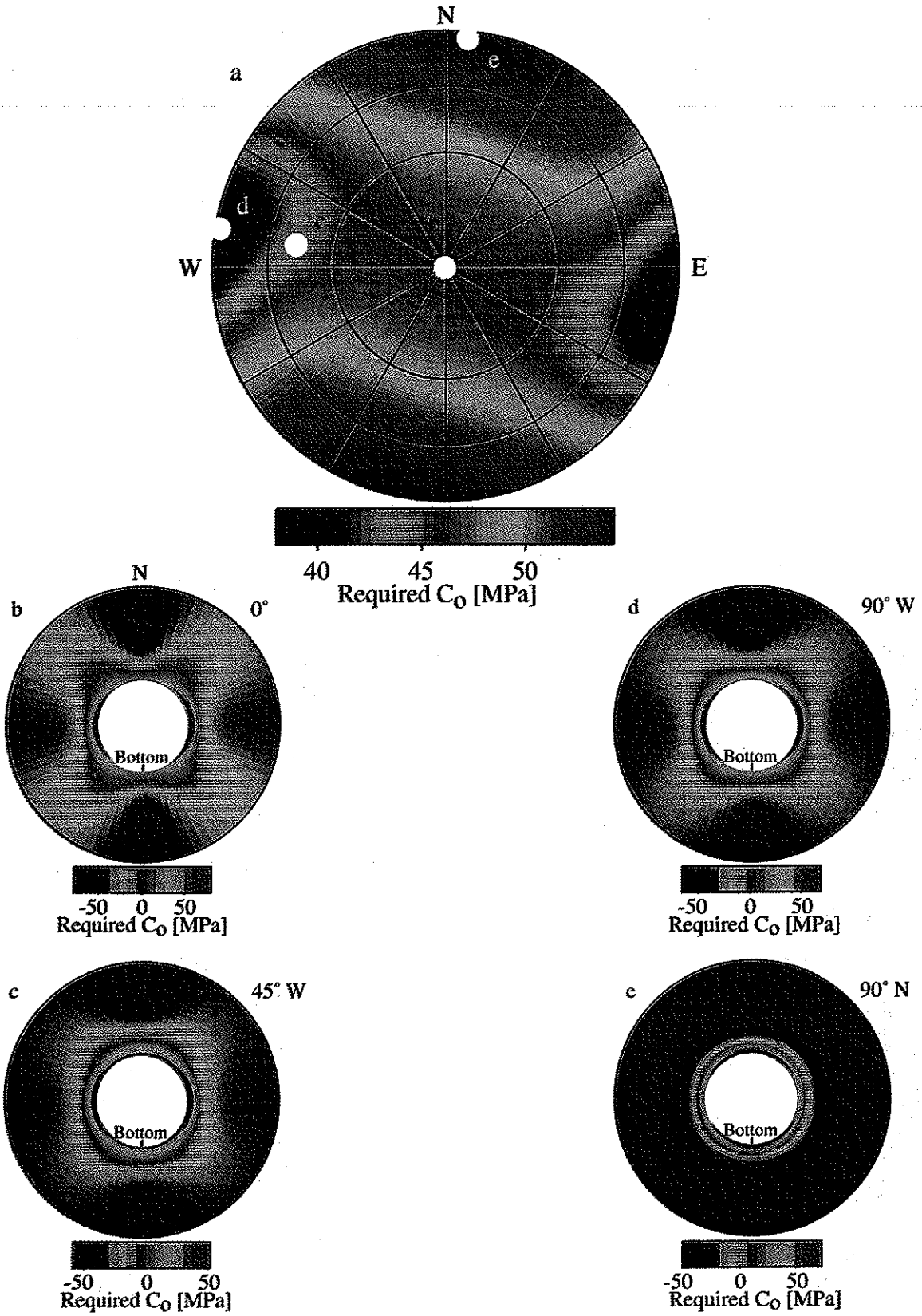

Fig. 10. (a) Stereonet showing the compressive rock strength needed to prevent wellbore failures after the pore pressure has been drawn down by 10 MPa and the horizontal stresses reduced by 6.5 MPa. The white points show the orientations of the wellbore cross-sections shown in parts (b–e). The colors correspond to the compressive rock strength needed to prevent failure in different parts of the rock surrounding the hole. (b) Vertical well. (c) Well inclined 45° at an azimuth of 280°. (d) Horizontal well drilled toward S_{Hmax}. (e) Horizontal well drilled toward S_{hmin}.

problems. Time was lost as a result of tight hole (i.e. hole pack-off, excessive overpull, or obstructions when running into the hole) and because of the extra time needed to ream the hole or circulate mud to clean cuttings from the bottom. Approximately 25% of the total downtime while drilling these holes was caused by hole-related, rather than equipment related, problems. Nearly 1200 cumulative hours of hole-related downtime, or approximately 10% of the total rig time, was lost on these holes. The time lost drilling these holes is almost equal to the time needed to drill well 5 to total depth of 3520 mTVD.

Compressive wellbore failures, if not controlled, may cause drilling problems like hole collapse, stuck pipe, pack-off, and obstructions when running into the hole, as well as problems while producing the reservoir such as sand production. Prevention of wellbore failure requires that the circumferential stresses around the wellbore be minimized. Fig. 8a shows a stereonet with the differential wellbore pressure ($\Delta P = P_m - P_p$) required to prevent compressive failures during drilling from growing beyond 90° in rock with 20 MPa uniaxial compressive strength. The stress state used in this analysis is the one found in the 10 S well at 2830 mTVD. Figs. 8b–e show cross-sections of wellbores for holes drilled in the directions shown in Fig. 8a, and assume a differential wellbore pressure of 6 MPa. The cross-sections are cut perpendicular to the axis of the wellbore and show the compressive rock strength needed to prevent the rock from failing and falling into the hole. A north arrow is shown in Fig. 8b for the vertical well, and the low side, or bottom, of the hole is shown if the well is inclined. Inclinations are shown next to each cross-section. As wells are increasingly inclined in the direction of the maximum horizontal stress (Figs. 8b–d), the compressive rock strength needed to prevent failure decreases. A well drilled in this stress field would experience problems if drilled vertically with an insufficient mud weight, and would experience fewer drilling problems as the well was inclined in the direction of the maximum horizontal stress. The most stable orientation is a wellbore drilled horizontally in the direction of the maximum horizontal stress because the nearly isotropic vertical and minimum horizontal stresses would not create large circumferential stress concentrations around the wellbore (Fig. 8d). If a well were drilled in the direction of the minimum horizontal stress it would encounter a stress field similar to that found in a well drilled vertically (Figs. 8b,e).

Well 10 S is deviated in the direction of the maximum horizontal stress, and it had the smallest amount of downtime of any well drilled in Visund. This well was also drilled with higher mud weights than were used in the previous eleven wells drilled in the field. The approach used in drilling this well is consistent with what we expect to be the best drilling strategy in Visund. The success of well 10 S compared to every well drilled before it serves to show that our strategy of increasing the mud weight and drilling in an optimal direction would have been effective in reducing drilling problems encountered in wells 1 through 9.

Fig. 9a shows the compressive rock strength needed to prevent breakouts from growing beyond 90° after the completion of drilling ($P = 0$), but before any pore pressure reduction has occurred. A wellbore drilled in the direction of the maximum horizontal stress would need compressive rock strengths as high as 30 MPa (Figs. 9a,d) in order to prevent significant wellbore failure. Because the uniaxial compressive rock strength in the reservoir sands is as low as 9–10 MPa in some sands (and as low as 15–25 MPa in others), we expect the onset of sand production problems in the weaker sands almost immediately after the initiation of production.

Fig. 10a shows the compressive rock strength needed to prevent breakouts from growing beyond 90° after the pore pressure in the reservoir has been drawn down by 10 MPa. We estimate the reduced horizontal stress by using a poroelastic model and a Poisson's ratio of 0.25, which reduces the horizontal stresses by 6.5 MPa [26]. The maximum horizontal stress is 65 MPa and the minimum horizontal stress is 46.7 MPa in this case. Even if the well is drilled in the optimal drilling direction we expect sand production to become significant as the reservoir is drawn down (Fig. 10d).

5. Conclusions

In this study we have shown that the full stress tensor can be reliably constrained using data that can be straightforwardly obtained as part of hydrocarbon field exploration and development. We demonstrate that in the Visund field, the maximum horizontal stress is significantly larger than the minimum horizontal and vertical stresses; and that our analysis is consistent with observations of recent deformation seen in studies of earthquakes and sub-seismic faults. We also show that the orientation of the stress tensor in this region is consistent both laterally and with depth.

Our analysis of wellbore stability illustrates that knowledge of stress magnitudes and orientations can be critical in designing successful exploration and production wells. By knowing the full stress tensor we are able to plan drilling strategies that minimize wellbore failure during drilling, and sand production while producing the reservoir. A significant reduction in the number of drilling problems and the amount of downtime of the rig was realized in well 10 S by modestly increasing the mud weight and by deviating the well in an optimally-stable direction.

Acknowledgements

We would like to thank Norsk Hydro for generously providing the data and financial support for this study.

Appendix A

Formation MicroImager data from taken from well 10 S are shown in Figs. A1–A4. These plots are "unwrapped" views of the wellbore with the azimuth from north shown along the top of each figure. The gray lines at an azimuth of approximately 270° show the pad 1 azimuth, and are used to orient the tool in the hole.

Appendix B

In wells 6, 8, 10 S, and 11 we observe sporadic occurrences of tensile fractures inclined with respect to the axis of the wellbore (Fig. 2). Because only well 10 S has a significant number of inclined fractures, we focus on this well. We split the inclined fractures into two sets, depending on the azimuth at which they formed (Fig. B1a). Fractures that formed at an azimuth of approximately 100° are gray, and those at approximately 300° are shown in black. There are fewer tensile fractures at 300° due to the keyseating in well 10 S, which tends to erode the tensile fractures. The azimuth of the data on this side of the hole is biased as a result, and does not show the expected average azimuth of 280°. Fig. B1b shows the inclination of the fractures as a function of depth. We measure the fracture inclination counter-clockwise from the downhole direction (insets of Fig. B1b). The fractures in this hole are typically inclined less than about 30° and more than about 150°. Fig. B1b shows that there is not a clear tendency for the fractures to be preferentially inclined in one direction. Fig. B1c shows the azimuth of the inclined

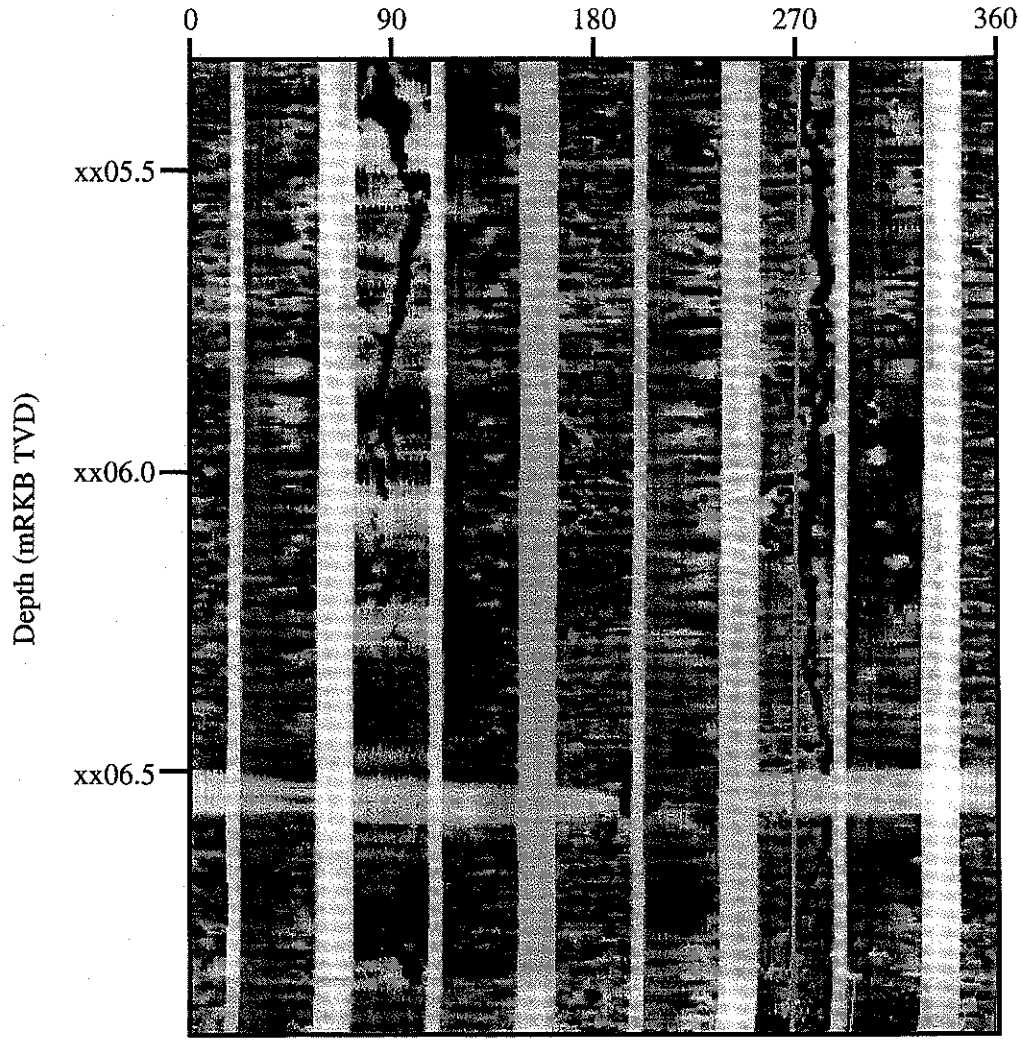

Fig. A1. FMI image of near-axial drilling-induced tensile wellbore failures. The tensile cracks appear at azimuths of approximately 90° and 270° in this plot. Note that the fractures are diametrically opposed, as we expect from theory.

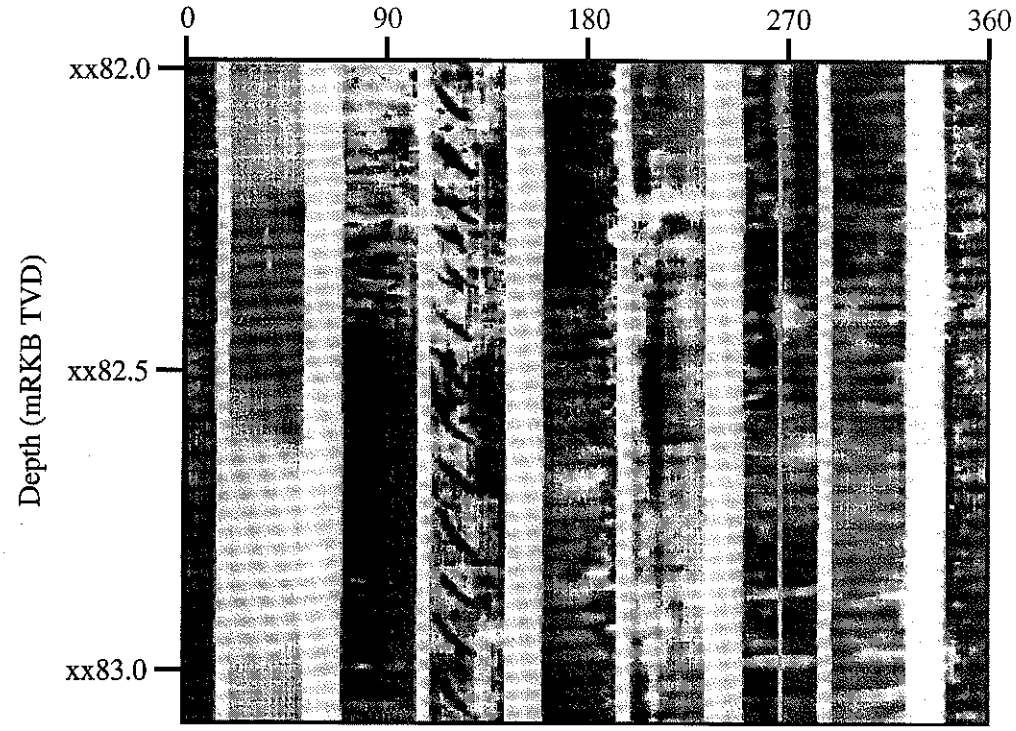

Fig. A2. FMI image of inclined drilling-induced tensile fractures. The tensile cracks appear at an azimuth of approximately 110° in this plot. No fractures are observed on the opposite side of the wellbore. This may be the result of poor image quality, reaming of the hole, or keyseating.

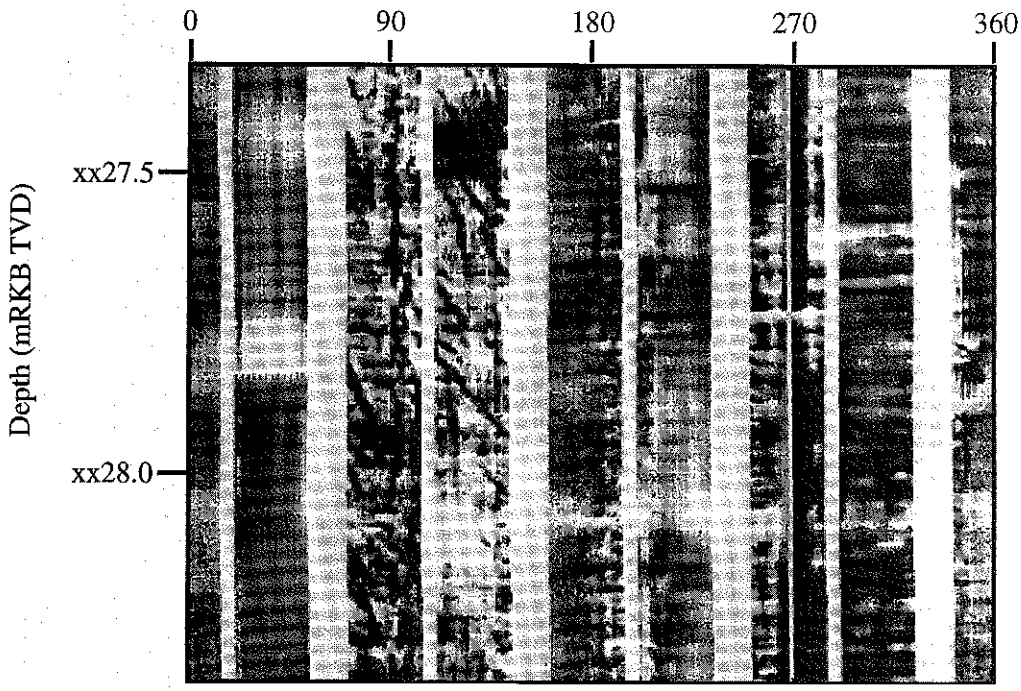

Fig. A3. FMI image of near-axial and inclined drilling-induced tensile fractures. The failures appear between approximately 80° and 110°. Some inclined fractures appear to grow into the near-axial fracture in this image. The dark band beneath the pad 1 azimuth is a keyseat, as the wellbore is deviated in this direction.

fractures plotted as a function of the inclination. The fractures generally fall into four groups. Each cluster represents fractures that have formed on the same side of the hole at similar inclinations. The fractures are rotated an average of approximately 25° from the axial orientation on both sides of the hole. The gray and black lines shown in the middle of the figure illustrate the simplified observations of the inclined tensile fractures in well 10 S. Inclined fractures formed at azimuths between 60° and 150° on one side of the hole, and between 270° and 340° on the opposite side. The inclinations of the tensile fractures range between near-axial fractures (0°) to 50° and from 115° back to near-axial fractures (180°).

We are able to reproduce the occurrence and orientation of the inclined tensile fractures shown in Fig. B1c using only minor perturbations to both the orientation of the stress tensor and the mud weight in well 10 S. Fig. B2 shows the expected minimum tangential (hoop) stress and corresponding fracture inclination (omega) as a function of the azimuth within the wellbore. The azimuth within the wellbore is defined as the angle measured clockwise from the bottom of an inclined well to a tensile or compressive failure.

In the first analysis we rotate S_{Hmax} 10° counter-clockwise (assuming a vertical principal stress), and increase ΔP by 3 MPa to a total of 9 MPa (Fig. B2a). Tensile fractures are expected to form when the minimum tangential stress falls below the tensile rock strength (zero stress) line. The gray shaded regions show the expected azimuths within the well where tensile fractures should form. Hatched areas along the omega axis show the possible inclinations for these fractures. Tensile fractures will form at any inclination between the two gray and the two black lines shown in the lower portion of the plot. These lines correspond to inclinations measured counter-clockwise from the downhole direction of approximately 155° and 25° for both the gray and black lines. The lines also correspond to azimuths within the well from about 165° to 185°, and from 345° to 5°. Because well 10 S is inclined to the west at an azimuth of 280°, fractures that form at azimuths within the well close to 0° and 180° (the low and high sides of the inclined hole) are

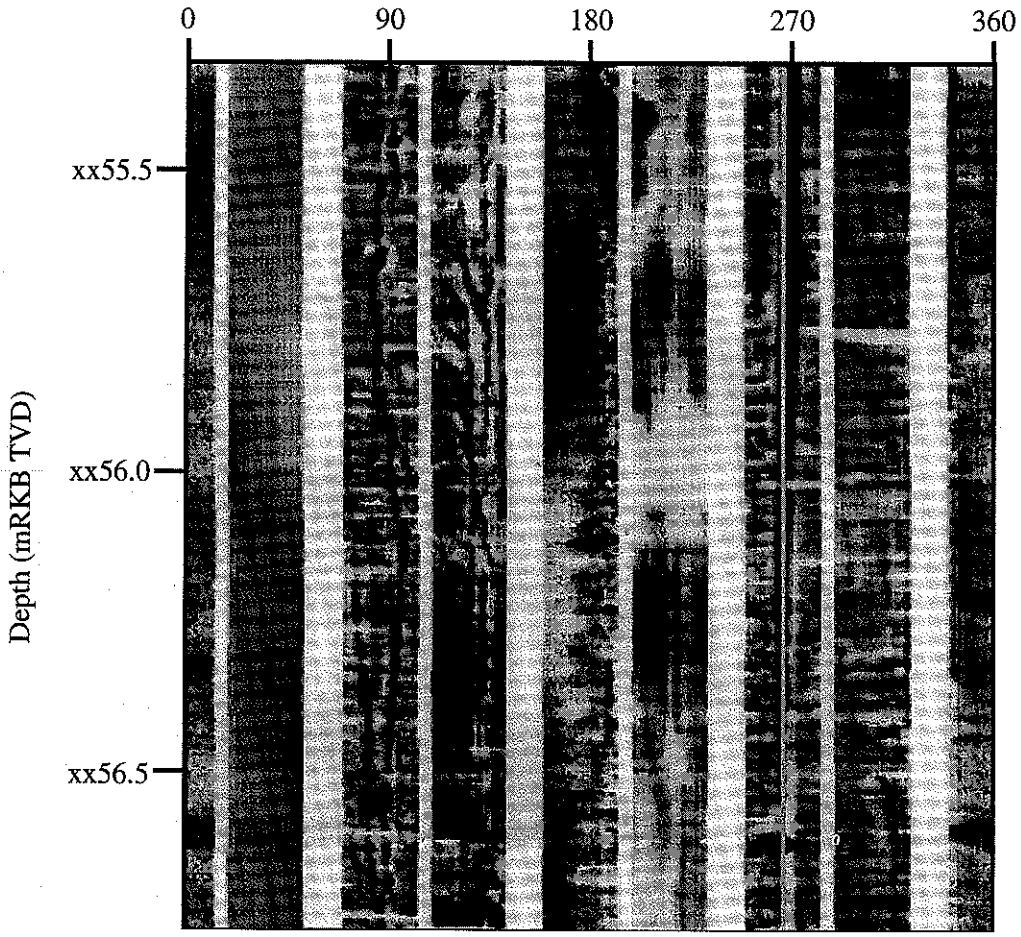

Fig. A4. FMI image of near-axial and inclined drilling-induced tensile fractures. The failures appear between approximately 90° and 120°. There may be a near-axial fracture at 120° that has inclined fractures growing toward the main axial fracture at 90°. A keyseat can be seen at 270°.

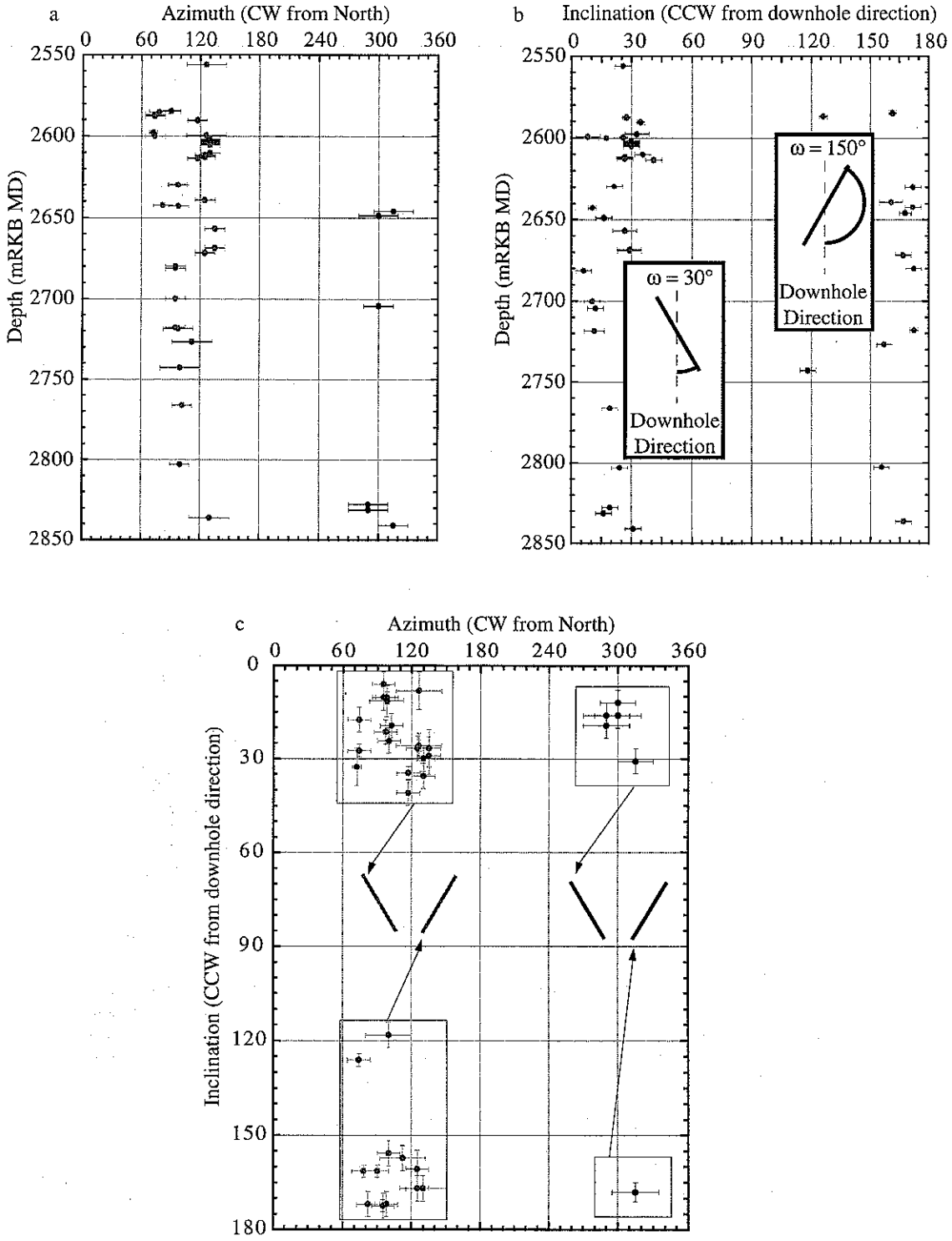

Fig. B1. (a) Azimuth of inclined fractures versus measured depth. The fractures are split into two groups depending on the side of the hole where they formed. (b) Inclination of fractures with respect to the downhole direction versus measured depth. The inclination of the fractures remains relatively small throughout the hole and has an average value of approximately 25° or 155°. (c) Azimuth of inclined fractures versus inclination measured counter-clockwise (ccw) from the downhole direction. The simplified observations are shown in the center of the plot.

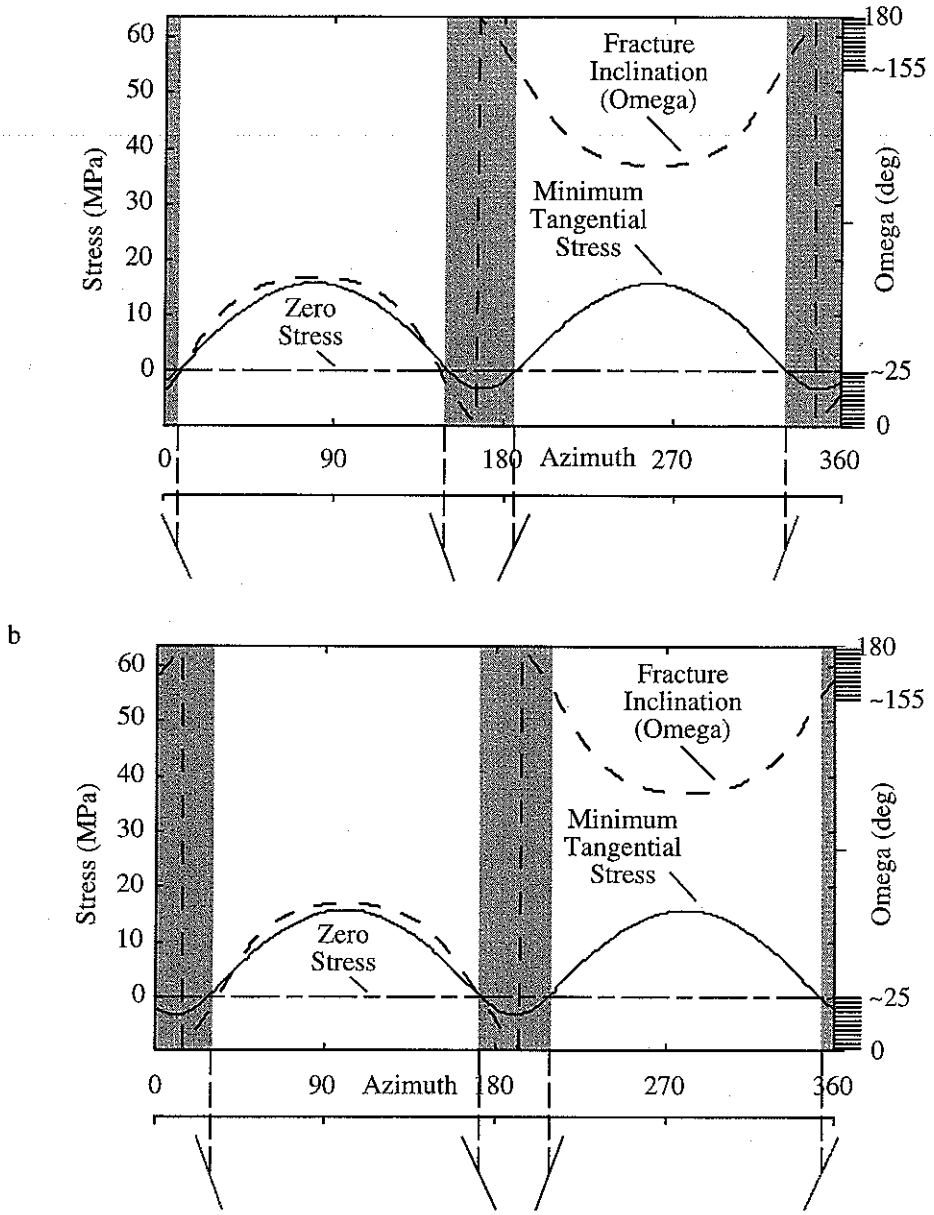

Fig. B2. (a) Minimum tangential stress (hoop stress) around the well for a stress state in which the maximum horizontal stress has been rotated 10° counter-clockwise. A slight increase in the differential fluid pressure of 3 MPa is used in this analysis. The gray and black lines below the plot show the expected range of orientations of the inclined tensile fractures. In this case, the fractures should be inclined less than 25° or more than 155° (gray and black lines respectively). (b) This plot is the same as in (a), except the maximum horizontal stress is rotated 10° clockwise.

in fact forming at azimuths measured from north of approximately 100° and 280°. Fig. B2b is the same as Fig. B2a, except the azimuth of S_{Hmax} is rotated 10° clockwise. This analysis provides similar results to those found from Fig. B2a. Thus, the stress state shown above for well 10 S predicts both the azimuth and inclination of the inclined tensile fractures, consistent with our observations from the FMI log.

The azimuth and inclination of the inclined tensile fractures can similarly be predicted by perturbing the vertical and minimum horizontal stresses. Therefore, the overall stress tensor can be accurately described with approximately vertical and horizontal principal stresses, however the orientation of the stress tensor clearly deviates from this approximation by small amounts.

References

[1] Lindholm CD, Bungum H, Villagran M, Hicks E. Crustal stress and tectoncis in Norwegian regions determined from earthquake

focal mechanisms. In: Proceedings of the Workshop on Rock Stresses in the North Sea, Trondheim, Norway, 1995.
[2] Færseth RB, Sjøblom TS, Steel RJ, Liljedahl T, Sauar BE, Tjelland T. Sequence Stratigraphy on the Northwest European Margin. Amsterdam: Elsevier, 1995.
[3] Müller B, Zoback ML, Fuchs K, Mastin L, Gregersen S, Pavoni N, Stephansson O, Ljunggren C. Regional patterns of tectonic stress in Europe. J Geophys Res 1992;97(B8):11,783–803.
[4] Gough DI, Bell JS. Stress orientations from borehole wall fractures with examples from Colorado, east Texas, and northern Canada. Can J Earth Sci 1981;19:1358–70.
[5] Zoback MD, Moos D, Mastin L, Anderson RN. Wellbore breakouts and in situ stress. J Geophys Res 1985;90:5523–30.
[6] Plumb RA, Hickman SH. Stress induced borehole elongation: a comparison between the four-arm dipmeter and the borehole televiewer in the Auburn geothermal well. J Geophys Res 1985;90:5513–21.
[7] Aadnoy BS. In situ stress direction from borehole fracture traces. J Pet Sci Eng 1990;4:143–53.
[8] Moos D, Zoback MD. Utilization of observations of well bore failure to constrain the orientation and magnitude of crustal stresses: application to continental, deep sea drilling project and ocean drilling program boreholes. J Geophys Res 1990;95(B6):9305–25.
[9] Brudy M, Zoback MD. Compressive and tensile failure of boreholes arbitrarily-inclined to principal stress axes: application to the KTB boreholes, Germany. International Journal of Rock Mechanics and Mining Sciences & Geomechanics Abstracts 1993;30(7):1035–8.
[10] Brudy M, Zoback MD. Drilling-induced tensile wall-fractures: implications for determination of in situ stress orientation and magnitude. Int. J. Rock Mech Min Sci & Geomech Abstr 1999; (in press).
[11] Zoback MD, Apel R, Baumgärtner J, Brudy M, Emmermann R, Engeser B, Fuchs K, Kessel W, Rischmüller H, Rummel F, Vernik L. Upper crustal strength inferred from stress measurements to 6 km depth in the KTB borehole. Nature 1993;365:633–5.
[12] Brudy M, Zoback MD, Fuchs K, Rummel F, Baumgaertner J. Estimation of the complete stress tensor to 8 km depth in the KTB scientific drill holes; implications for crustal strength. JGR 1997;102-8:18,453–75.
[13] Ekstrom MP, Dahan CA, Chen MY, Lloyd PM, Rossi DJ. Formation imaging with microelectrical scanning arrays. In: Transactions of the SPWLA Annual Logging Symposium, 27. 1986. p. BB1–BB21.
[14] Mardia KV. In: Statistics of directional data. New York: Academic Press, 1972. p. 357.
[15] Fejerskov M. Determination of in situ rock stresses related to petroleum activities on the Norwegian continental shelf. Doctoral Thesis: Department of Geology and Mineral Resources Engineering, Norwegian University of Science and Technology, 1996.
[16] Shamir G, Zoback MD. Stress orientation profile to 3.5 km depth near the San Andreas Fault at Cajon Pass, California. J Geophys Res 1992;97(4):5059–80.
[17] Barton CA, Zoback MD. Stress perturbations associated with active faults penetrated by boreholes; possible evidence for near-complete stress drop and a new technique for stress magnitude measurement. J Geophys Res 1994;99(5):9373–90.
[18] Paillet FL, Kim K. Character and distribution of borehole breakouts and their relationship to in situ stresses in deep Columbia River Basalts. J Geophys Res 1987;92(7):6223–34.
[19] Borgerud L, Svare E. In-situ stress field on the Norwegian Margin, 62°–67° north. In: Proceedings of the Workshop on Rock Stresses in the North Sea, Trondheim, Norway, 1995.
[20] Peska P, Zoback MD. Compressive and tensile failure of inclined well bores and determination of in situ stress and rock strength. J Geophys Res 1995;100(B7):12,791–811.
[21] Gaarenstroom L, Tromp RAJ, de Jong MC, Brandenburg AM. Overpressures in the Central North Sea: implications for trap integrity and drilling safety. In: Parker JR, editor. Geology of Northwest Europe: Proceedings of the 4th Conference, 1993. p. 1305–13.
[22] Byerlee JD. Friction of Rocks. Pure and Applied Geophysics 1978;116:615–29.
[23] Wiprut DJ, Zoback MD, Peska P, Hanssen TH. Constraining the full stress tensor from observations of drilling-induced tensile fractures and leak-off tests: application to borehole stability and sand production on the Norwegian margin. Int J Rock Mech Min Sci 1997;34(34) Paper No. 00365.
[24] Vernik L, Bruno M, Bovberg C. Empirical relations between compressive strength and porosity of siliciclastic rocks. Int J Rock Mech Min Sci & Geomech Abstr 1993;30(7):677–80.
[25] Jørgensen T, Bratli RK. In situ stress determination and evaluation at the Tampen Spur area. In: Proceedings of the Workshop on Rock Stresses in the North Sea, Trondheim, Norway, 1995.
[26] Engelder T, Fischer MP. Influence of poroelastic behavior on the magnitude of minimum horizontal stress, Sh, in overpressured parts of sedimentary basins. Geology 1994;22:949–52.